

# A Comparative Study Structural Models, Lattice Planes, and Patterson Densities in Three Polymorphs of Titanium Dioxide

Neetu<sup>1</sup>and Satish Kumar<sup>1</sup>

<sup>1</sup>Department of Physics, OPJS University, Churu, Raj., India

## ABSTRACT

Titanium dioxide,  $TiO_2$ , is one of the most important bio-compatible material and photocatalytic material that exist as three main polymorphs anatase, rutile, and brookite. The presence one or all of these polymorphs phases can significantly affect the overall performance of the material. In current study, we explore the main difference structural models, lattice parameters, and Patterson densities of all three polymorphs using Visualization for Electronic and Structural Analysis (VESTA) theoretical tool. An illustration of the intense Lattice planes that appear in five different  $TiO_2$  polymorphs is also presented. The Patterson densities were analyzed by using model electron densities and model nuclear densities and constructed structure models are attributed to various phases of  $TiO_2$  polymorphs.

## 1. INTRODUCTION:

In the last few decades, Titanium dioxide which is also known as Titania, attracts the attention of numerous researchers due to its capability to work as a photocatalyst and help in many technological and eco-friendly applications. Titanium dioxide has a diverse application area including hydrogen generate, treating air and water pollution, blocking pigments as well as biological areas and display and sensor technologies, photocatalytic, photocatalysis, light-energy conversion systems, paints, papers, sunscreen, and ultraviolet (UV) [1-3]. Various structures of  $TiO_2$  such as mesoporous nanorods, nanotubes, and core-shell structures with the hybrid materials have also been established in particular appropriate for solar cell electrode capability and photocatalysis [4]. Over the existing fourteen polymorphs of  $TiO_2$  the anatase, rutile, and brookite phases have been extensively studied. The crystallographic structure of  $TiO_2$  observed to occur in different phases called transition polymorphs. The cell volume of brookite- $TiO_2$  is bigger as compared anatase or rutile- $TiO_2$ , having eight  $TiO_2$  groups in one unit cell in comparison to four for anatase- $TiO_2$  and two for rutile- $TiO_2$ . The rutile- $TiO_2$  exhibit furthermost refractive indices in visible region of electromagnetic spectrum in comparison to other known crystal, which makes it a potential candidate for specific optical instrument based on polarization optics with working range longer visible and infrared region [5-8]. The phase-dependent crystallographic study on polymorphs of  $TiO_2$  is, therefore, essential to understanding the coordination environments as well as the distribution of electrons and nucleons. Numerous theoretical approaches for predicting the crystal structure have been established but they are not suitable for displaying inter-atomic distances and bond angles. To analyze the variation in band gap for anatase, brookite, and rutile-

TiO<sub>2</sub> polymorphs, it is necessary to visualize their fundamental structures and geometrical structure factors. The current research work aims to distinguish between the three main polymorphs of titanium dioxide.

## 2. COMPUTATIONAL DETAIL

The investigation of crystallographic information in language of structure models, lattice planes, ranges of fractional coordinates, and Patterson densities form model electron densities and model nuclear densities of TiO<sub>2</sub> polymorphs, in particular anatase, brookite, and rutile is performed by VESTA software theoretical tool using the available observed values (as Listed in Table.1).

## 3. RESULTS AND DISCUSSIONS

The anatase, rutile and brookite phases of TiO<sub>2</sub> are selected from numerous polymorphs for the comparative investigation of crystallographic parameters using structure models, lattice planes, ranges of fractional coordinates and analysis of Patterson densities by applying concept of model electron densities and model nuclear densities.

### 3.1. STRUCTURE MODELS

An organized investigation for the crystallographic information using structure models of three polymorphs of TiO<sub>2</sub> (especially anatase, rutile, and brookite) in five different styles are compared and explored by using VESTA theoretical tool and demonstrated in Fig.1. Both anatase and rutile have a tetragonal crystal system while brookite having orthorhombic. The values of lattice parameters *a* and *b* increase while that of *c* observed to decreases as we move in order anatase rutile and brookite respectively.

**Table.1.** Polymorphs-TiO<sub>2</sub> structure with their crystallographic parameters

Polymorphs TiO <sub>2</sub>	Crystal system	Space group (No.)	Lattice parameters			Unit cell volume (Å <sup>3</sup> )
			<i>a</i> (Å)	<i>b</i> (Å)	<i>c</i> (Å)	
anatase-TiO <sub>2</sub>	tetragonal	I4 <sub>1</sub> /amd (141)	3.77	3.77	9.48	134.73
brookite-TiO <sub>2</sub>	orthorhombic	Pbca (61)	9.19	5.46	5.15	258.41
rutile-TiO <sub>2</sub>	tetragonal	P4 <sub>2</sub> /mnm (136)	4.58	4.58	2.95	61.88

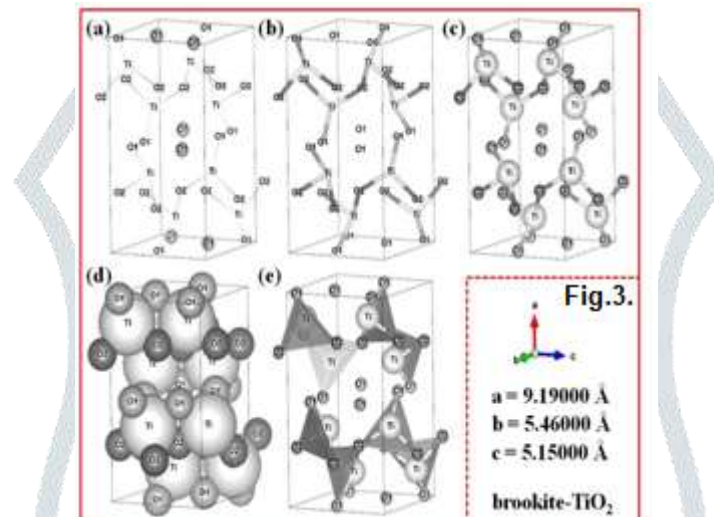
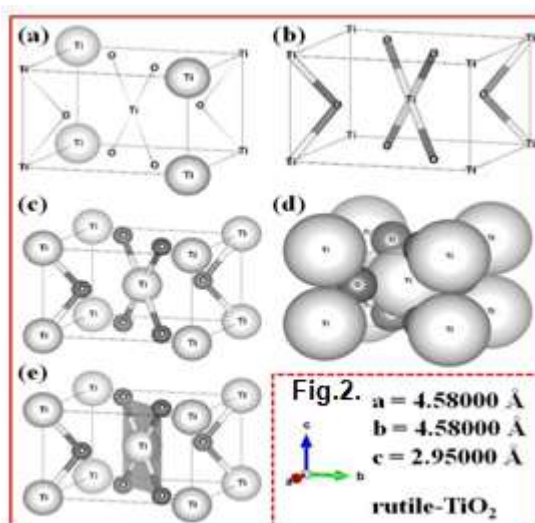
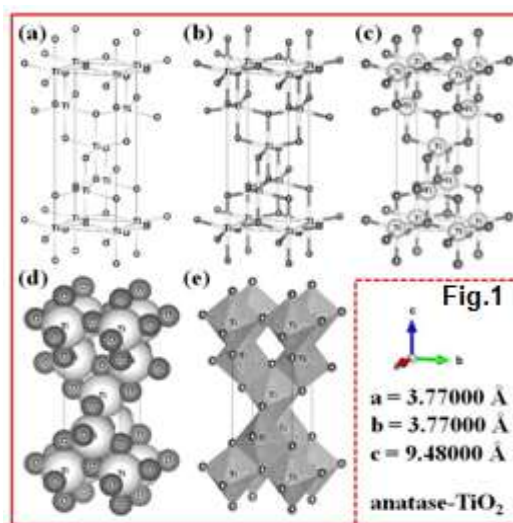


**Fig. 1-3. Crystallographic representation: anatase, rutile and brookite(a) wire-frame, (b) stick, (c) ball stick, (d) space-filling (e) polyhedral structural models of Anatase, Rutile, and Brookite respectively. Colour code: gray and small spheres indicate oxygen (O) atoms; white and large spheres point out the titanium (Ti) atoms, polyhedra are showing in gray color.**

### 3.2. LATTICE PLANES

The wireframe structure models of dominant lattice planes appear in various phases; particularly anatase, rutile, and brookite phase of  $\text{TiO}_2$  polymorphs from a crystallographic perspective are shown and discussed in Fig.2. (a-c) provides the crystallographic representation of dominant lattice planes (101) and (200) that appear in anatase- $\text{TiO}_2$  polymorphs structure. The densest lattice planes (210) and (321) observed in brookite- $\text{TiO}_2$  polymorphs are displayed in Fig. 2(b). Fig. 2(c) illustrates the crystallographic demonstration of the intense lattice planes (110) and (211) observed in rutile- $\text{TiO}_2$  polymorphs structure [9-12].

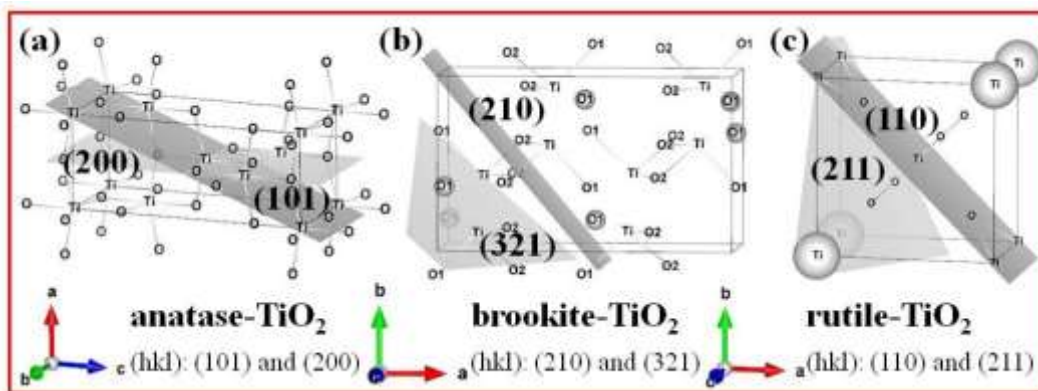


**Fig.2.(a-c)** Crystallographic representation of the intense Lattice Planes in  $\text{TiO}_2$  polymorphs: (a) anatase- $\text{TiO}_2$ , (b) brookite- $\text{TiO}_2$  and (c) rutile- $\text{TiO}_2$ . All the lattice planes are described by a set of integer Miller indices (hkl). The representative unit cell is enveloped using thin solid lines in the wireframe structure model.

### 3.3. Lattice Planes and Ranges of Fractional Coordinates

A comparative study on the visualization of lattice planes family and ranges of fractional coordinates of different polymorphs of  $\text{TiO}_2$ ; in particular anatase, rutile and brookite  $\text{TiO}_2$  polymorphs is performed and displayed in Fig. 3-5.

The dissimilar lattice planes of anatase phase of  $\text{TiO}_2$  are shown by Fig.3. (a-c) confirms using by different set Miller indices (hkl). Fig. 3.(a) explore the lattice planes along the z-direction *i.e.* (001), (002) and (003), whereas the lattice planes along the y-direction *i.e.* (010), (020) and (030) are demonstrated in Fig.3.(b) and (100), (200) and (300) lattice planes along the x-direction are displayed in Fig.3.(c). Fig.3. (d-g) reveals the fractional coordinates ranges of anatase. Fig.3. (d)  $x = y = z = 1$ , hence it's have one unit cell, even as Fig.3. (e) Demonstrate  $y = z = 1$ ,  $x = 2$  presenting one extra unit cell in x-direction. Likewise in Fig.3 (f)  $x = z = 1$ ,  $y = 2$  indicating one extra unit cell along y-direction and Fig.3. (g),  $y = z = 1$ ,  $x = 2$  also observed to have one extra unit cell along z-direction [13-15].

Fig.4.(a-g) grant the visualization of the various lattice planes for rutile-phase of  $\text{TiO}_2$  having dissimilar Miller indices (hkl) values. The lattice plane shown in Fig.4 (a) are (100), (110) and (120) in Fig.4. (b) (010), (011) and (012) and (100), (101) and (102) sketching in Fig.4. (c) For rutile- $\text{TiO}_2$ . Fig.4. (d-g) also explores the fractional coordinates ranges. Fig.4.(d) indicate the wireframe structure model having position  $x = y = z = 1$ , providing only one unit cell of rutile  $\text{TiO}_2$ , while Fig.4. (e) Reveals  $y = z = 1$  and  $x = 2$  referring one extra unit cell along x-direction. Same way the Fig. 4.(f), showing position  $x = z = 1$  but  $y = 2$ , also one extra unit cell but along y-direction and finally Fig.4.(g) with  $x = y = 1$  but  $z = 2$  [16-19], showing one extra unit cell in z-direction.

The various kinds of lattice planes of brookite-polymorphs of  $\text{TiO}_2$  are shown by Fig.5(a-g) with diverse set of Miller indices (hkl) values. Fig.5. (a-c) explore the different sets of lattice planes (100), (200) and (400), Fig.5. (b) (010), (020) and (040) and Fig.5.(c). (001), (002) and (004) lattice planes are illustrated in Fig.5.(d-g) explore the ranges of fractional coordinates of brookite-polymorphs of  $\text{TiO}_2$ . Fig.5. (d) with positional parameters  $x = y = z = 1$  having single unit cell while Fig.5.(e) shows  $x = z = 1$  but  $y = 2$  have one extra unit

cell along y-direction. In same manner, Fig.5.(f) having positional parameters  $x = y = 1$  but  $z = 2$ , clearly indicating one extra unit cell along z-direction and Fig.5.(g) owing position  $y = z = 1$  but  $x = 2$  also revealing one extra unit cell in x-direction [20-21].

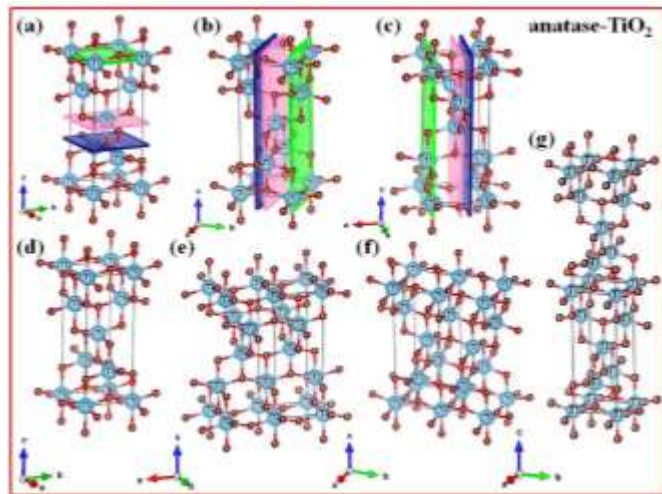


Fig.3(a-g) Crystallographic representation Anatase TiO<sub>2</sub>

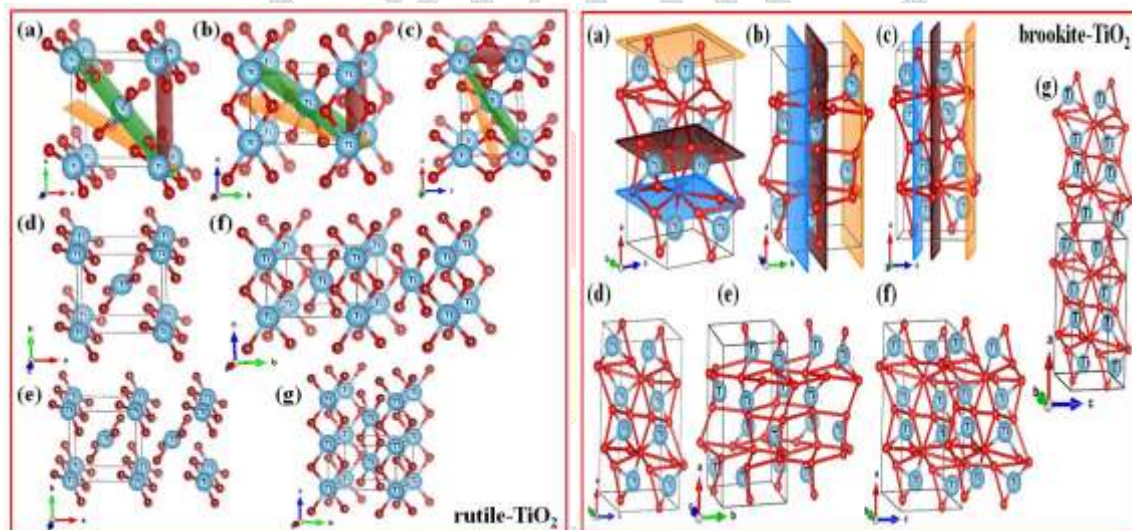


Fig.4(a-g) Crystallographic representation

Rutile TiO<sub>2</sub>

Fig.5(a-g) Crystallographic representation

Brookite Ti

### 3.4.PATTERSON DENSITIES

An organized investigation on the crystallographic data for Patterson densities from model electron densities and model nuclear densities of three polymorphs of TiO<sub>2</sub> (especially anatase, rutile, and brookite) is compared and established using VESTA theoretical tool, as shown in Fig.6.(A-C). The crystallographic structural characteristics of anatase-TiO<sub>2</sub> are represented in Fig.6.A.(a-c). The wireframe structure model of anatase TiO<sub>2</sub> was observed to crystallize in a tetragonal crystal system. The isolated TiO<sub>2</sub> molecule is evident in Fig.6.A.(a), where each oxygen (O) atom is shared with three titanium (Ti) atoms and each Ti atom shared with six oxygen atoms further confirming the formation of the anatase-TiO<sub>2</sub>. The bond length between Ti and O atoms is 1.9795 Å, which corresponds to the standard bond-length of metal and oxygen atoms.

Fig.6A.(b) stand for the model electron density of anatase-TiO<sub>2</sub>, while green and red/orange shaded portion showing the electron density of Ti and O atoms, [22-25]. The shaded green segment is bigger than the red/orange shaded portion verifying the Ti atom has a bigger electron density as in comparison to O atom. Fig.6A.(c) disclose the the anatase-TiO<sub>2</sub>model nuclear density, where small shaded portions of Patterson density using model nuclear density are visible in this form of image.

Fig.6.B.(a-c) displays the representative wireframe structure model of the rutile-TiO<sub>2</sub> structure. To explain the crystal structure of rutile-TiO<sub>2</sub>, the tetragonal unit cell is often more convenient containing titanium (Ti) and oxygen (O) atoms, where each O atom is shared with two Ti atoms and each Ti atom shared with four O atoms. The calculated bond-length between Ti and O atoms is about 1.9462 Å, which is well-matched with the established results. The Patterson densities observed from model electron density and model nuclear density are depicted in Fig.6.B.(a) to Fig.6.B. (c), respectively.

The crystallographic form in terms of structure model and Patterson densities of brookite-TiO<sub>2</sub> is shown in Fig.6(C).(a-c). Fig.6.C.(a) illustrates the wireframe representative structure model of brookite-TiO<sub>2</sub>, corresponding to an orthorhombic crystal system. The isolated TiO<sub>2</sub> molecule is visible in Fig.6.C(b), where each titanium (Ti) atom is shared with two oxygen (O) atoms (O1 and O2) verifying the formation of the brookite-TiO<sub>2</sub>. The bond-length between Ti and O atoms is about 1.9365 Å and 1.9246 Å for O1 and O2 atoms, respectively. The observed bond-lengths are well-matched with the established results [26-30]. Fig.6.C.(b) represents the model electron density of brookite-TiO<sub>2</sub>. Fig6.C.(c) exhibit the model nuclear density of brookite-TiO<sub>2</sub>. The oxygen atoms are linked with the other unit cell.

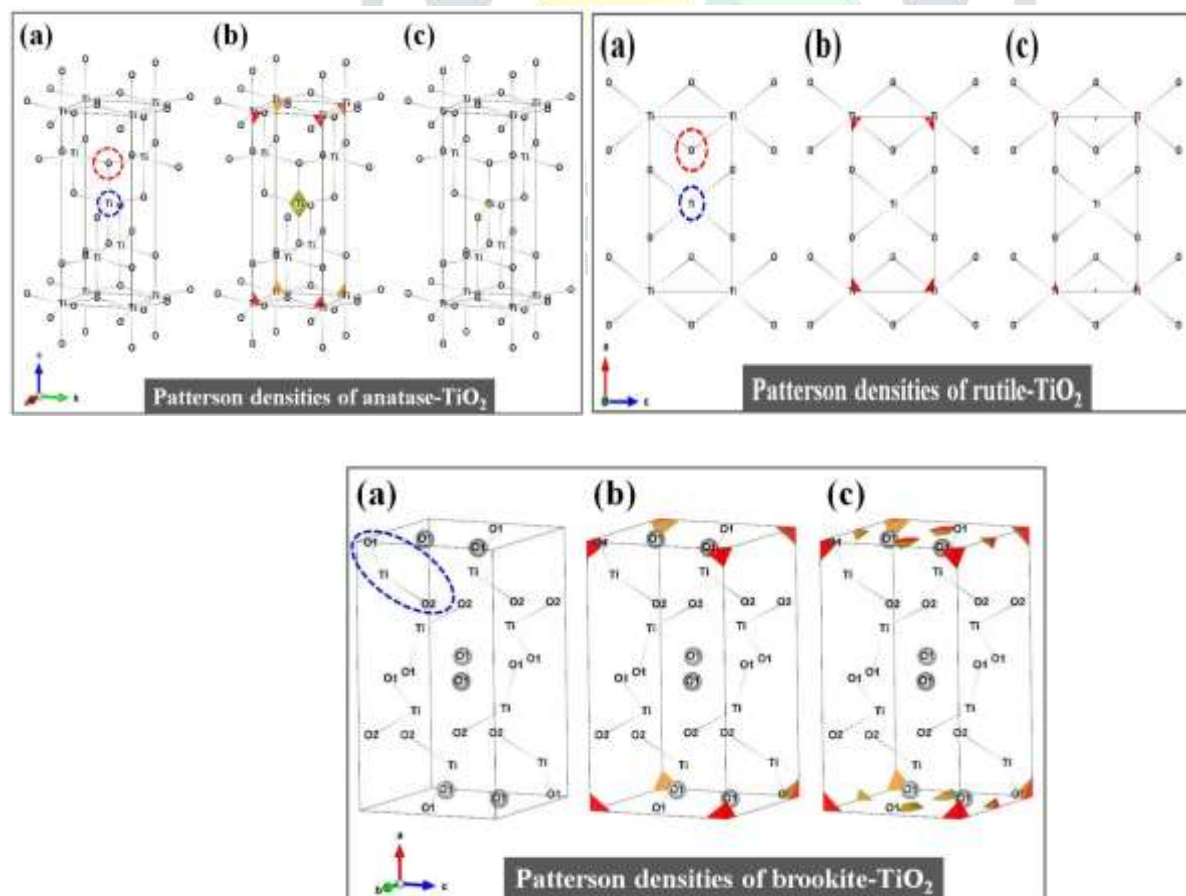


**Fig.6(A-C) Crystallographic representation of Anatase,Rutile and Brookite-TiO<sub>2</sub>**

**Table.2.**The atomic position of Titanium and Oxygen atoms in Anatase, Rutile and Brookite - $\text{TiO}_2$ 

<b>TiO<sub>2</sub></b>	<b>Atom</b>	<b>X</b>	<b>y</b>	<b>z</b>	<b>bond length (Å)</b>
<b>Polymorphs</b>					
anatase- $\text{TiO}_2$	titanium (Ti)	0.000	0.000	0.000	Ti-O → 1.979
	oxygen (O)	0.000	0.000	0.208	
brookite- $\text{TiO}_2$	titanium (Ti)	0.128	0.098	0.862	Ti-O1 → 1.936
	oxygen (O1)	0.011	0.147	0.182	Ti-O2 → 1.938
	oxygen (O2)	0.229	0.108	0.534	
rutile- $\text{TiO}_2$	titanium (Ti)	0.000	0.000	0.000	Ti-O → 1.946
	oxygen (O)	0.305	0.305	0.000	

#### 4. Conclusions

The investigation of different lattice and structural parameters including lattice planes, ranges of fractional coordinates and Patterson densities from model electron densities and model nuclear densities for different  $\text{TiO}_2$  polymorphs structures are successfully done. By using VESTA theoretical tool, the bond lengths of titanium atoms with oxygen atoms for different polymorphs  $\text{TiO}_2$  structures are calculated. The two important Patterson densities, especially model electron density and model nuclear density, are compared and visualized through VESTA theoretical tool on three titania polymorphs structures. The investigation of phase-dependent Patterson density suggests the general importance of anatase, rutile, and brookite  $\text{TiO}_2$  in both fundamental and application-oriented research.

#### References:

1. J. Gangwar, B. K. Gupta, S. K. Tripathi and A. K. Srivastava, *Nanoscale* **7**, 13313(2015).
2. M. Niu, F. Huang, L. Cui, P. Huang, Y. Yu, and Y. Wang, *ACS Nano* **4**, 681 (2010).
3. C. C. Yang, and Y. W. Mai, *Mater. Sci. Eng. R* **79**, 1 (2014).
4. M. I. Khan, *J. Solid State Chem.* **152**, 105 (2000).
5. J. Gangwar, B. K. Gupta and A. K. Srivastava, *Defence Sci. J.* **66**, 323-340 (2016).
6. Y. Li, M. Gecevicius, and J. Qiu, *Chem. Soc. Rev.* **45**, 2090 (2016).
7. R. Asahi, T. Morikawa, T. Ohwaki, K. Aoki, and Y. Taga, *Science* **293**, 269 (2001).
8. K. K. Dey, D. Bhatnagar, A. K. Srivastava, M. Wan, S. Singh, R. R. Yadav, B. C. Yadav and, M. Deepa, *Nanoscale* **7**, 6159 (2015).
9. S. Zhang, L. Ren, and S. Peng, *Cryst. Eng. Comm.* **16**, 6195 (2014).
10. Q. J. Xiang, J. G. Yu, and M. Jaroniec, *Chem. Soc. Rev.* **41**, 782 (2012).
11. S. Li, S. Xu, L. He, F. Xu, Y. Wang, and L. Zhang, *Polym.-Plast. Technol. Eng.* **49**, 400 (2010).

12. J. Gangwar, K. K. Dey, S. K. Tripathi, M. Wan, R. R. Yadav, R. K. Singh, Samta and A. K. Srivastava, *Nanotechnology* **24**, 415705 (2013).

13. M. Y. Xing, Y. M. Wu, J. L. Zhang, and F. Chen, *Nanoscale* **2**, 1233 (2010).

14. C. Y. Flores, C. Diaz, A. Rubert, G. A. Benitez, M. S. Moreno, M. A. F. L. De Mele, R. C. Salvarezza, P. L. Schilardi, and C. Vericat, *J. Colloid Interface Sci.* **350**, 402 (2010).

15. T. Froschl, U. Hormann, P. Kubiak, G. Kucherova, M. Pfanzelt, C. K. Weiss, R. J. Behm, N. Husing, U. Kaiser, K. Landfester and M. W. Mehrenes, *Chem. Soc. Rev.* **41**, 5313-5360 (2012).

16. R. Verma, J. Gangwar, and A. K Srivastava, *RSC Adv.* **7**, 44199 (2017).

17. Z. Ren, E. Kim, S. W. Pattinson, K. S. Subrahmanyam, C. N. R. Rao, A. K. Cheetham, and D. Eder, *Chem. Sci.* **3**, 209 (2012).

18. J. F. Jacobs, L. V. de Poel, and P. Osseweijer, *Nanoethics* **4**, 103 (2010).

19. H. Zhang and J. F. Banfield, *Chem. Rev.* **114**, 9613-9644 (2014).

20. M. Gratzel, *Nature* **414**, 338 (2001).

21. D. C. Sayle, J. A. Doig, S. A. Maicanianu, and G. W. Watson, *Phys. Rev. B: Condens. Matter Mater. Phys.* **65**, 245414 (2002).

22. K. Liu, M. Cao, A. Fujishima, and L. Jiang, *Chem. Rev.* **114**, 7740 (2014).

23. J. Yao, M. Yang and Y. Duan, *Chem. Rev.* **114**, 6130-6178 (2014).

24. J. Gangwar, A. Chandran, T. Joshi, R. Verma, A. M. Biradar, S. K. Tripathi, B. K. Gupta, and A. K. Srivastava, *Mater. Res. Express* **2**, 075013 (2015).

25. L. Poul, S. Ammar, N. Jouini, F. Fievet, and F. Villain, *Solid State Sci.* **3**, 31 (2001).

26. M. Cargnello, T. R. Gordon, and C. B. Murray, *Chem. Rev.* **114**, 9319 (2014).

27. Ebelmen, *Ann. Chim. Phys. Ser.* **57**, 319 (1846).

28. S. Shang, K. Xue, D. Chen, and X. Jiao, *Cryst. Eng. Comm.* **13**, 5094 (2011).

29. J. Gangwar, B. K. Gupta, P. Kumar, S. K. Tripathi, and A. K. Srivastava, *Dalton Trans.* **43**, 17034 (2014).

30. Y. Zhou, and M. Antonietti, *J. Am. Chem. Soc.* **125**, 14960 (2003).